

Supplementary Information

**Aggregation-driven fluorescence quenching of imidazole-functionalized perylene diimide for
urea sensing**

Junghyun Cho, Changjoon Keum, Sang-Guk Lee and Sang-Yup Lee*

1. Color changes of the PDI-Hm solution and UV at high methanol volume fraction

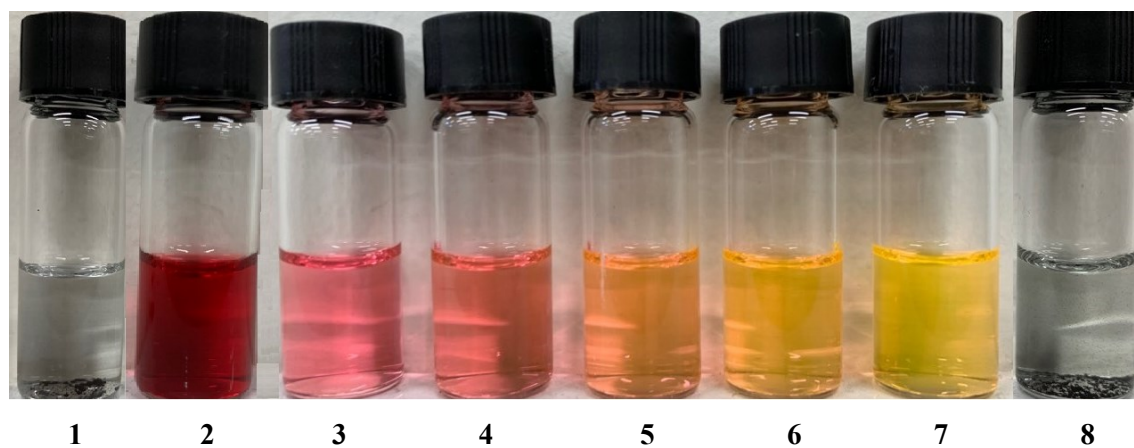


Fig. S1. Colours of the PDI-Hm solutions in 0.01N HCl-MeOH mixture at various methanol volume fractions (φ). Samples are as follows; **1:** H₂O 100% (insoluble, without HCl), **2:** $\varphi = 0.0$, **3:** $\varphi = 0.1$, **4:** $\varphi = 0.3$, **5:** $\varphi = 0.5$, **6:** $\varphi = 0.7$, **7:** $\varphi = 0.9$, **8:** $\varphi = 1.0$ (insoluble).

2. Solubility of PDI-Hm at high methanol volume fraction

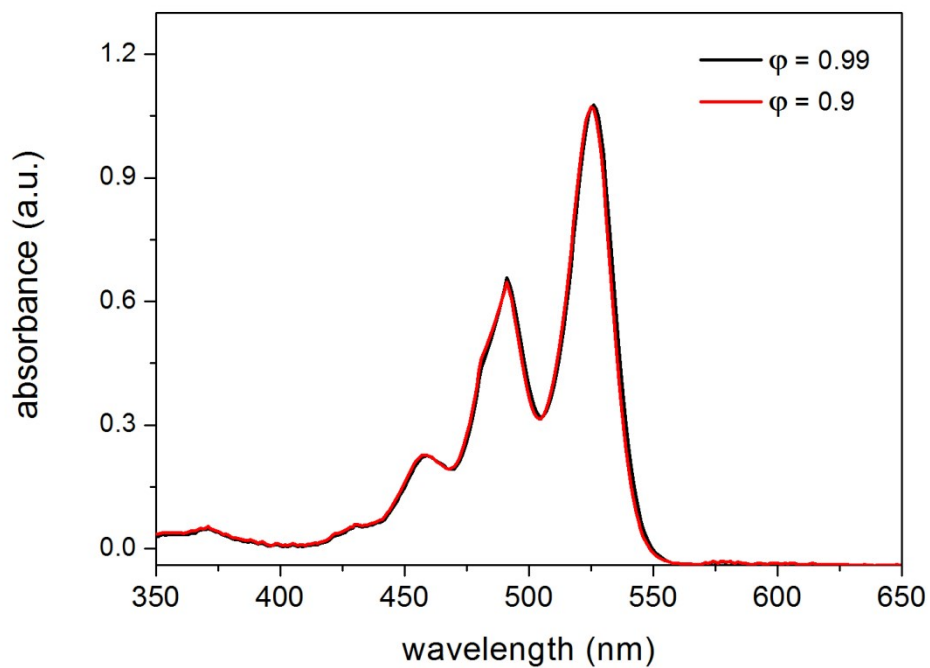


Fig. S2. Agreement of UV-Vis spectra at methanol-rich mixtures of $\varphi = 0.9$ and 0.99 .

3. Calculation of the stability ratio (W)

For the theoretical analysis on the aggregation of PDI-Hm in the HCl-methanol mixture, the stability ratio (W) was calculated with the consideration of van der Waals attraction potential (Φ_{att}) and electrical repulsion potential (Φ_{rep}). The stability ratio, W , is expressed as a function of the distance of x between two PDI-Hm molecules in the form of Eq. (1).¹

$$W(x) = 2 \int_{2L_C}^{\infty} e^{\Phi(x)/kT} \frac{1}{x^2} dx \quad (1)$$

$$\Phi(x) = \Phi_{att} + \Phi_{rep} \quad (2)$$

By introducing a dimensionless parameter of s , defined by Eq. (4), Eq. (1) is expressed as Eq. (3).

$$W(s) = 2 \int_0^{\infty} e^{\Phi(s)/kT} \frac{1}{(s+2)^2} ds \quad (3)$$

where,

$$s = \frac{x - 2L_C}{L_C} \quad (4)$$

For the calculation of the attraction potential, Hamaker constant, H , was estimated with considerations of PDI-Hm and solvent properties using the Lifshitz theory given in Eq. (5)².

$$H_{131} = \frac{3}{4} kT \left(\frac{\varepsilon_1 - \varepsilon_3}{\varepsilon_1 + \varepsilon_3} \right)^2 + \frac{3h\nu_e}{16\sqrt{2}} \frac{(n_1^2 - n_3^2)^2}{(n_1^2 + n_3^2)^{3/2}} \quad (5)$$

where, k is Boltzmann constant, ε_i is dielectric constant of component i , n_i is refractive index of component i , h is Planck's constant, ν_e is the main electronic absorption frequency set as $3 \times 10^{15} \text{ s}^{-1}$. Components of $i = 1$ and 3 represent PDI-Hm and the solvent (HCl-methanol mixture at various volumetric ratio), respectively. The dielectric constant of PDI-Hm (ε_1) was assumed to be 2.87, same to that of naphthalene⁴, since exact value of PDI-Hm could not be obtained. Dielectric constants of the HCl-methanol mixture (ε_3) were evaluated from the linear regression of the experimental data in literature⁵. Refractive index of PDI-Hm (n_1) was set as 1.530⁶, whereas refractive indices of the HCl-methanol mixture at various volume contents was approximated from the fifth order of polynomial fitting curve of data in a reference (Fig. S3)⁷. Using these values of the solvent and PDI-Hm, Hamaker constants were calculated. Dielectric constants, refractive indices and Hamaker constants of water-methanol mixture are summarized in Table S1. Degree of the protonization of imidazole (f) was assessed from the potentiometry. The cell potentials (E) of the imidazole solutions (2 mM) and blank solutions (i.e. without imidazole) of the HCl-methanol mixture at various volumetric ratios were measured. The cell potential was measured using a pH meter equipped with a glass pH electrode (Ross Orion 8103BNUWP, Thermo Scientific). The potential difference between imidazole and blank solutions provides activity ratio (a_0/a_H) based on Nernst equation (Eq. 6)⁸;

$$E = E^0 + 59.14 \log a \quad \text{at STP} \quad (6)$$

where, E^0 is standard potential and a is the activity of proton in solution.

From Eq. (6) the cell potentials of blank and imidazole solutions are

$$E(\text{blank}) = E^0 + 59.14 \log a_0 \quad (6-1)$$

$$E(\text{imidazole}) = E^0 + 59.14 \log a_H \quad (6-2)$$

Thus, the potential difference of $E(\text{blank})$ and $E(\text{imidazole})$ is Eq. (7).

$$E(\text{blank}) - E(\text{imidazole}) = \log \left(\frac{a_0}{a_H} \right) \quad (7)$$

In Eq (6) and (7), a_0 and a_H represent the activities of proton in blank and imidazole solutions, respectively. The activity ratio of a_0/a_H was converted to the degree of protonation (f) by Eq. (8).

$$f = 1 - \frac{a_H}{a_0} \quad (8)$$

All potentiometric measurements were performed at 25°C and cell potentials were determined from the average value ($n = 3$).

Degree of the protonation of imidazole evaluated from the comparison of the activities is shown in Table S1 and Fig. S4.

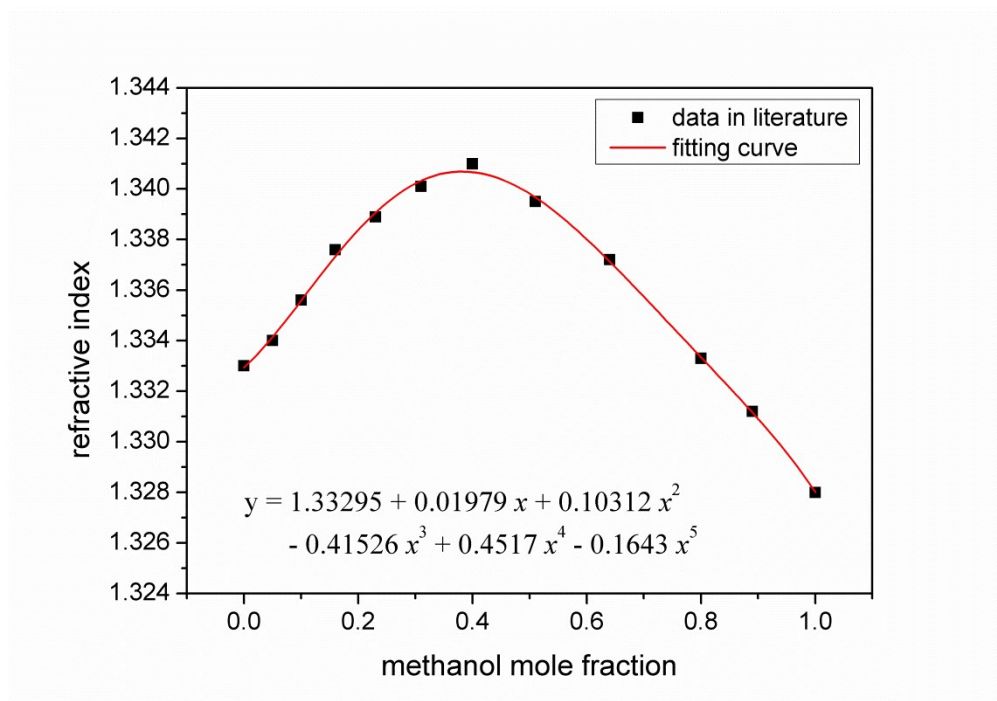


Fig. S3. Data fitting curve of the refractive index of water-methanol mixture. Experimental data set was obtained from reference 6.

Table S1. Dielectric constants, refractive indices, Hamaker constants and degree of protonation of water-methanol mixture

HCl:Methanol volume ratio	Dielectric const. of solvent (ϵ_3)	Refractive index of solvent (n_3)	Hamaker const. ($\times 10^{20}$ J)	Degree of protonation (f)*
10:0	78.480	1.333	1.271	0.655
9:1	75.049	1.334	1.261	0.596
7:3	67.520	1.336	1.232	0.566
5:5	59.058	1.339	1.194	0.565
3:7	49.557	1.341	1.171	0.576
9:1	38.810	1.335	1.214	0.486

* f is determined from the potentiometry.

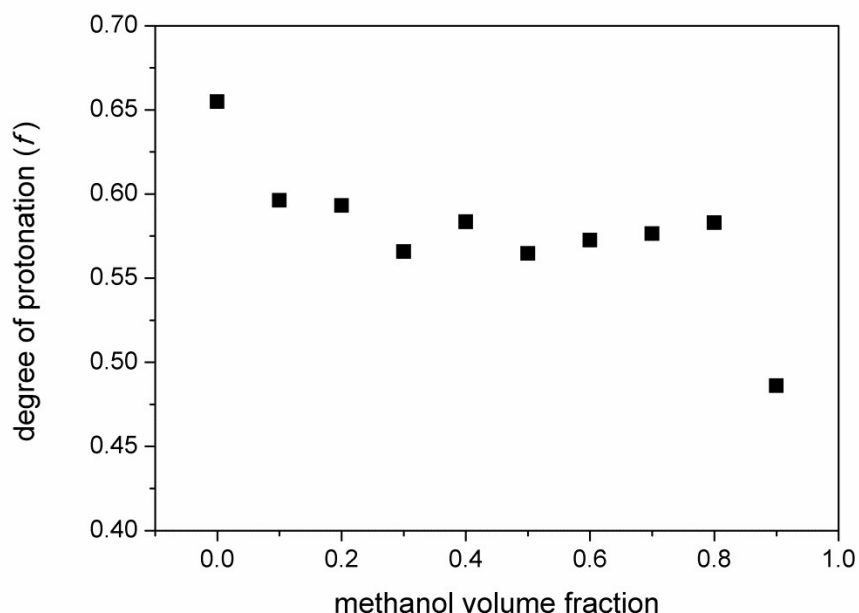


Fig. S4. Degree of protonation of imidazole in HCl-methanol mixture

References

- 1 R. R. P. C. Hiemenz, *Principles of Colloid and Surface Chemistry, Revised and Expanded*, CRC Press, 2016.
- 2 J. Israelachvili, *Intermolecular & Surface Forces*, Academic Press, London, UK, 2nd Ed., 1991.
- 3 R. R. P. C. Hiemenz, *Principles of Colloid and Surface Chemistry*, Marcel Dekker, New York, USA, 3rd Ed., 1997.
- 4 K. Ishii, M. Kinoshita and H. Kuroda, *Bull. Chem. Soc. Jpn.*, 1973, 46, 3385–3391.
- 5 P. S. Albright and L. J. Gosting, *J. Am. Chem. Soc.*, 1946, **68**, 1061–1063.
- 6 Z. Kişnişçi, Ö. F. . F. Yüksel and M. Kuş, *Synth. Met.*, 2014, **194**, 193–197.

- 7 A. Ripin, S. K. Abdul Mudalip and R. Mohd. Yunus, *J. Teknol.*, 2008, **48**, 61–73.
- 8 N. Aslan, P. E. Erden, A. Doğan, E. Canel and E. Kılıç, *J. Solution Chem.*, 2016, **45**, 299–312.

4. Critical concentration of hydroxide

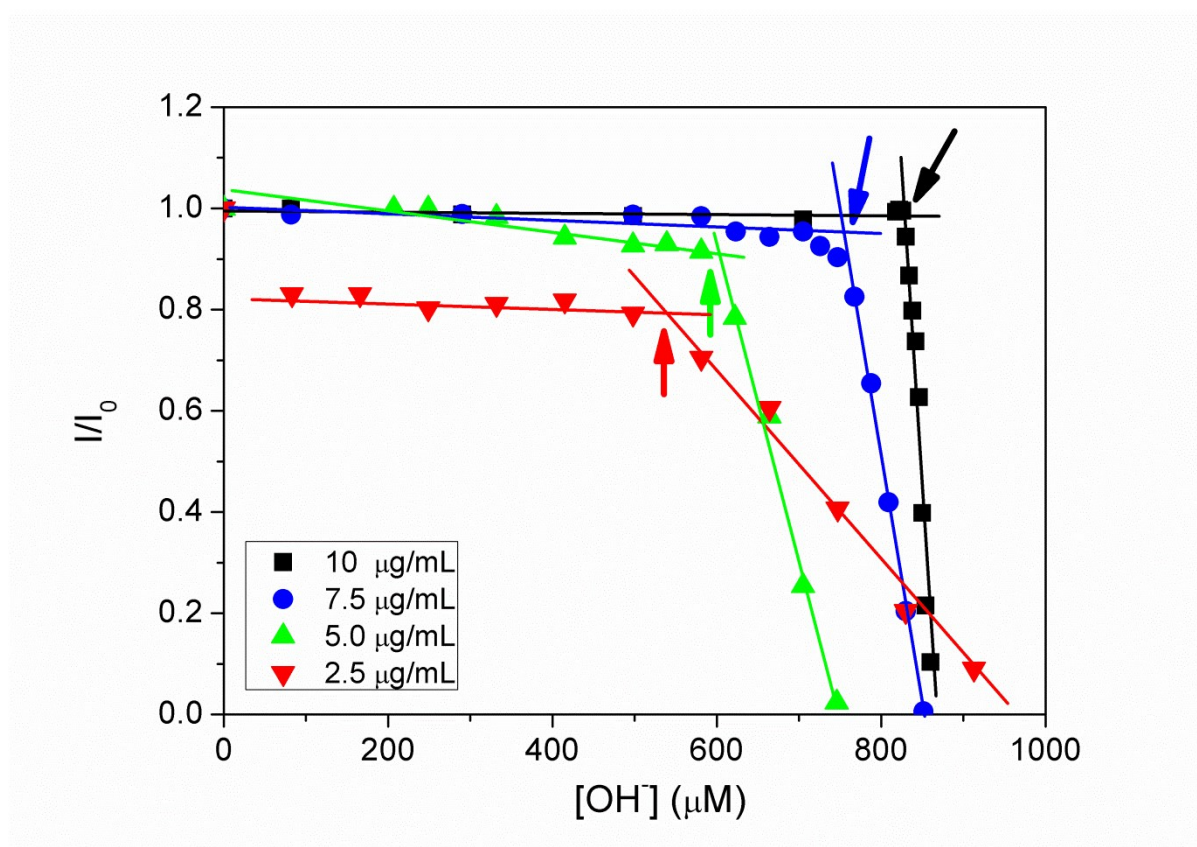


Fig. S5. The critical concentrations of hydroxide are marked by arrows at which drastic intensity of PDI-Hm change occurs. The critical points were determined from the cross point of the linear regression lines.

5. Changes of the critical concentration with respect to the PDI-Hm concentrations

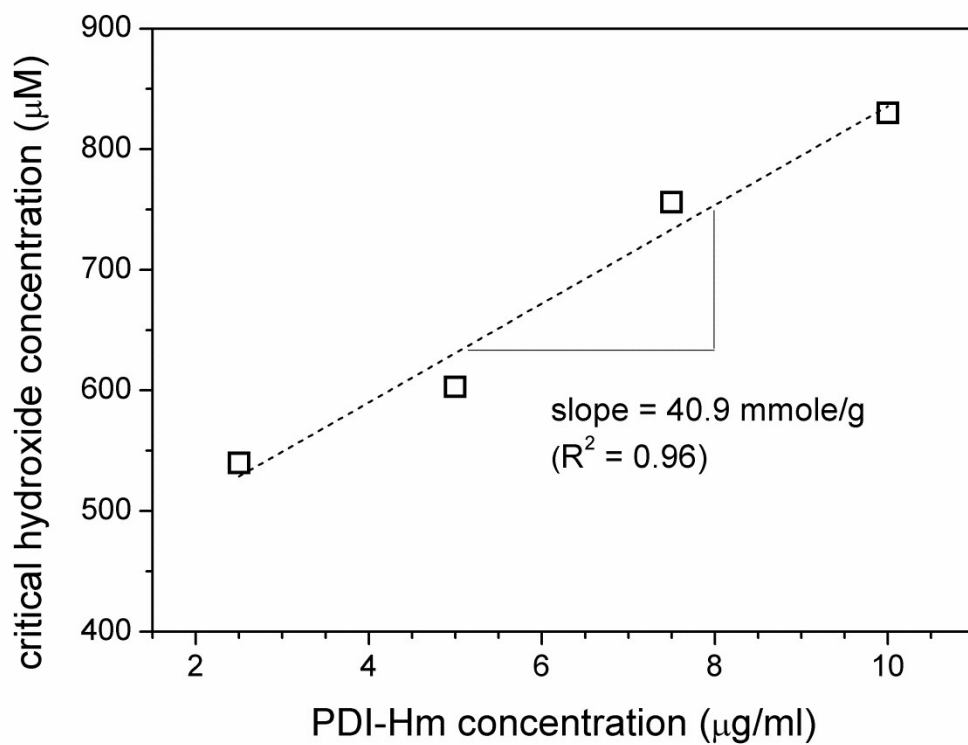


Fig. S6. Change of the critical concentration of hydroxide with increasing PDI-Hm concentration.

6. Shift of excitation peak with PDI-Hm concentration

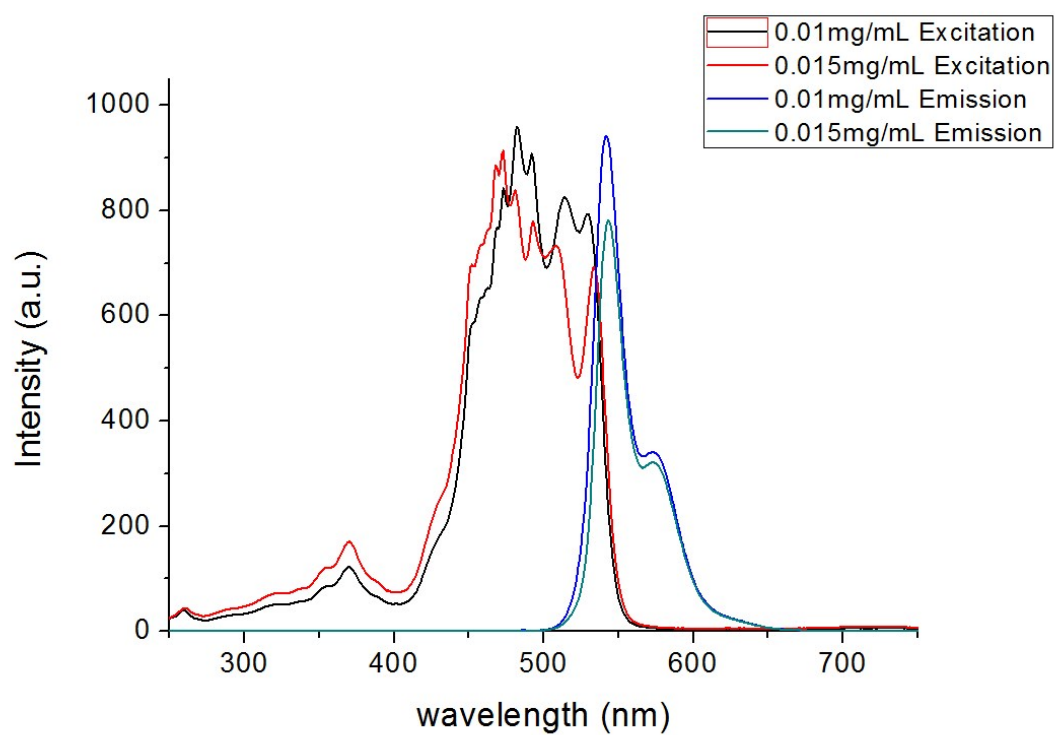
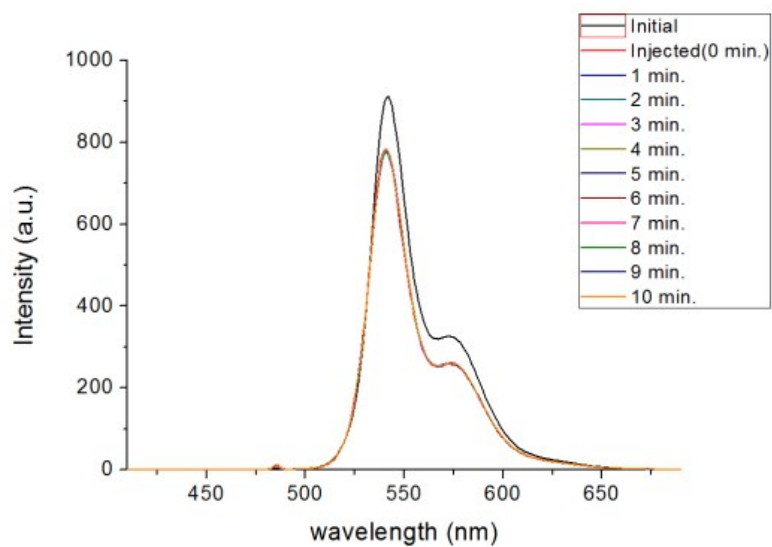
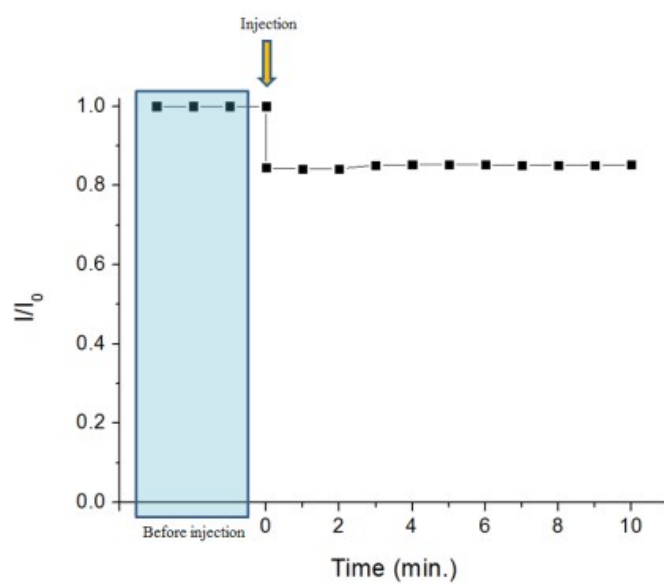


Fig. S7. Excitation spectral shift occurred at a concentration of 0.015mg/mL. In addition, the emission intensity has been reduced.

7. Evaluation of the response time



(a)



(b)

Fig. S8. Response time of PDI-Hm solution to hydroxide. (a) Fluorescence spectra scanned before/after addition of OH^- , (b) Fluorescence intensity change with time.

8. Optimization of the reaction conditions

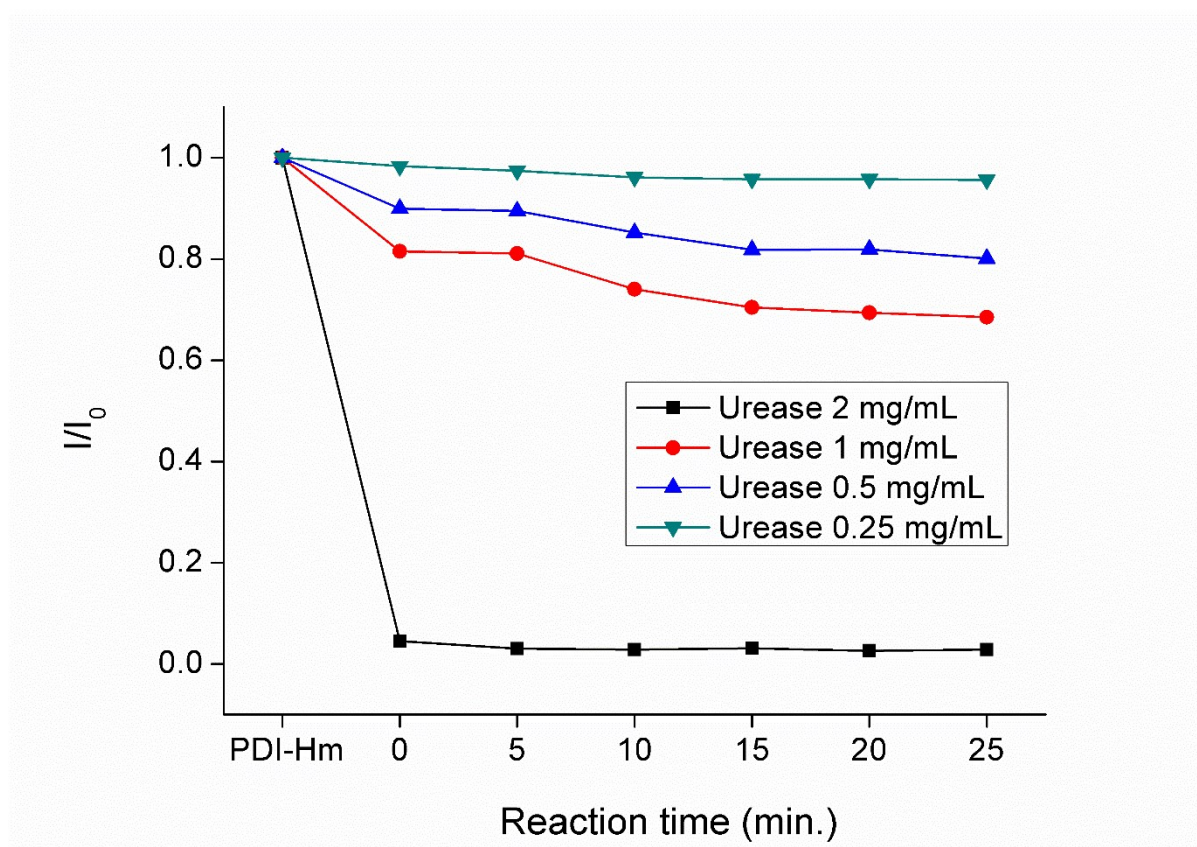


Fig. S9. Fluorescence change with variations of the urease concentration and reaction time. PDI-Hm indicates the fluorescence intensity without any reactant. For the urea hydrolysis, 2 mM urea solution was applied for the urea hydrolysis.

9. Comparison with other sensors

Table S2. Comparison with other sensing methods

Type	Sensing system	Linear range(mmol/L)	Detection limit (mmol/L)	Response time	Ref.
Covalent binding, PVC-COOH polymer	Potentiometric	0.1-10	0.1	1-2 min.	1
Entrapment, triacetyl cellulose membrane	Optical	1-500	1	1-5 min.	2
Poly(n-butyl acrylate)	Fluorescence	0.1-100	-	30 min.	3
Acrylic microspheres Reflectometry	Reflectometry	0.01-1000	0.01	10 min.	4
Imidazole-functionalized perylene diimide	Fluorescence	0.4-10	0.4	<1 min.	This work

[1] M. Gutiérrez, S. Alegret and M. del Valle, *Biosens. Bioelec.*, 2007, 22, 2171–2178.

[2] M. Krysteva and M. Al Hallak, *ScientificWorld Journal*, 2003, 3, 585–592.

[3] W. Ngeontae, C. Xu, N. Ye, K. Wygladacz, W. Aeungmaitrepirom, T. Tuntulani and E. Bakker, *Anal. Chim. Acta*, 2007, 599, 124–133.

[4] A. Ulianas, L. Y. Heng and M. Ahmad, *Sensors*, 2011, 11, 8323–8338.

10. Scheme of PDI-Hm xerogel film sensor

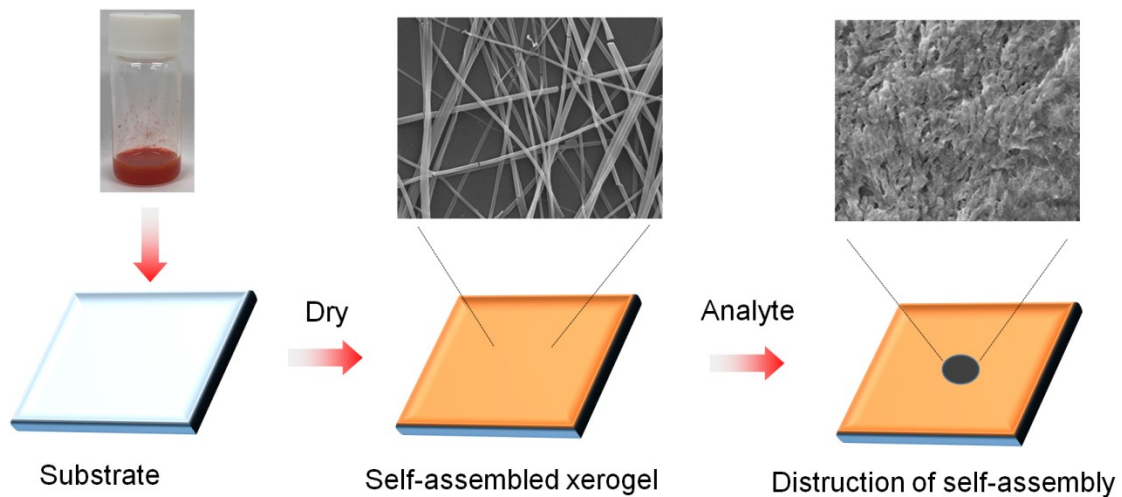


Fig. S10. Schematic illustration of PDI-Hm self-assembled gel film sensor. The fibrous rigid self-assembled structure is destroyed by the added basic analyte, losing fluorescence and turning black.

11. The fluorescence spectra of the PDI-Hm gel

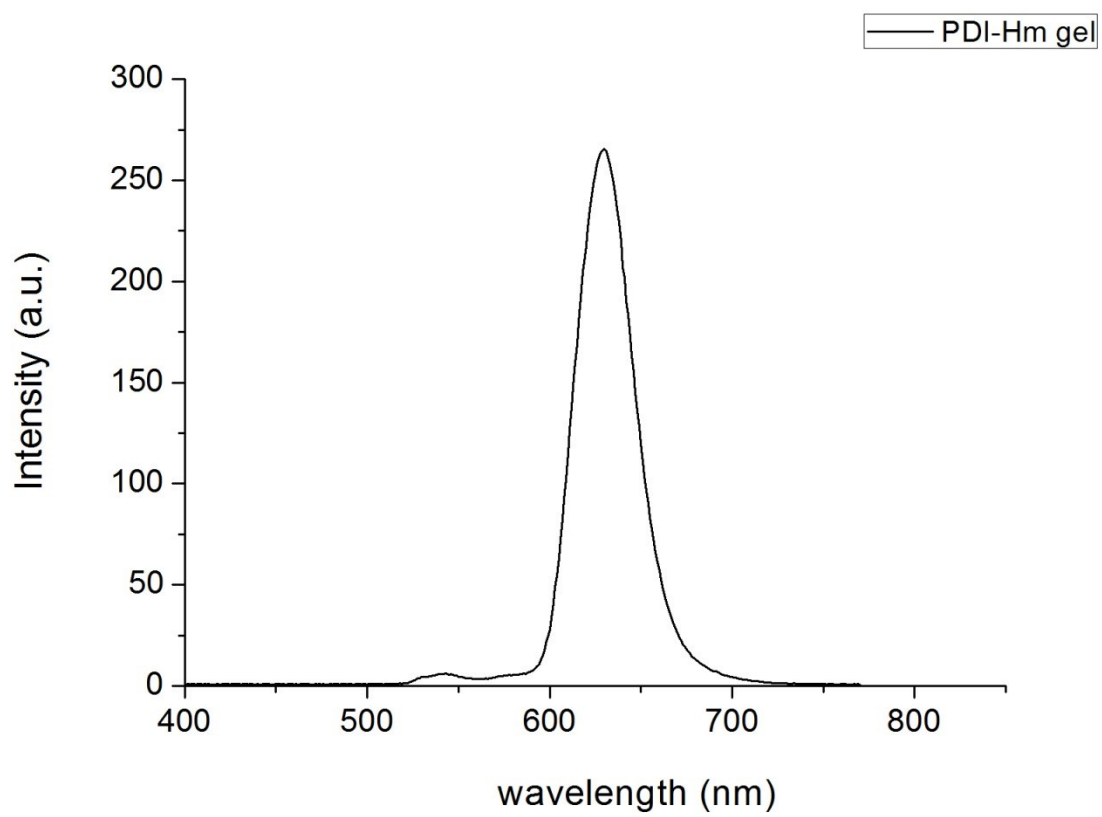


Fig. S11. The fluorescence spectra of PDI-Hm gel. $\lambda_{\text{ex}} = 526\text{nm}$, $\lambda_{\text{em}} = 630\text{nm}$.

12. PDI-Hm aggregates formed by the coffee ring effect

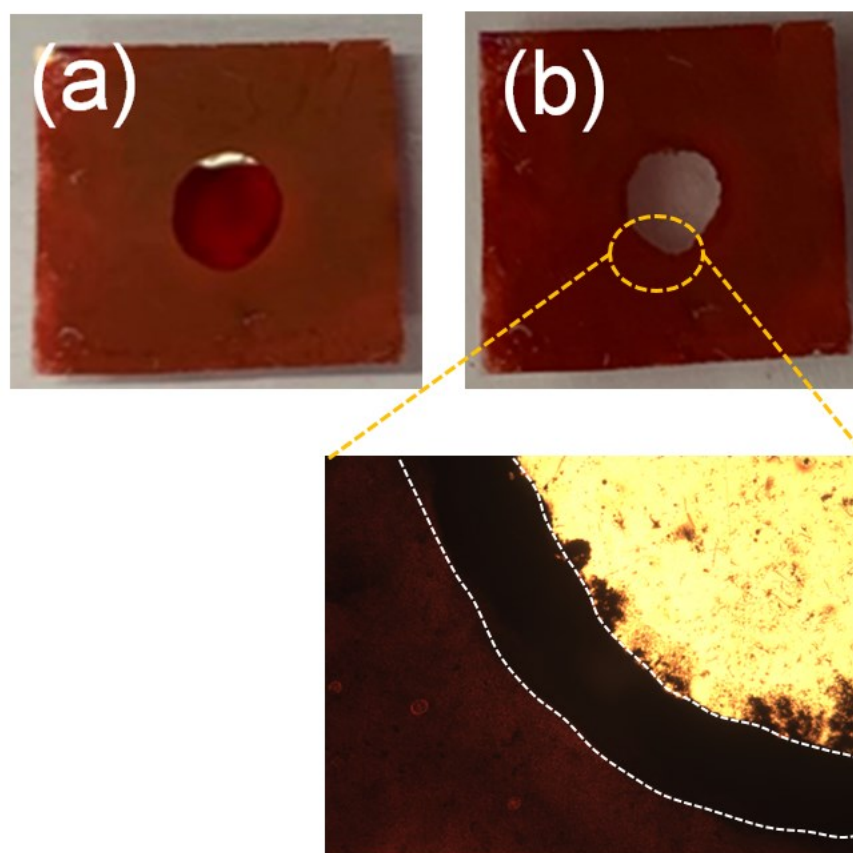


Fig. S12. Photo images of the hole on the PDI-Hm gel film. (a) Right after dropping the hydrolyzed urea solution lower than 10 mM, (b) After evaporation, PDI-Hm molecules were moved to the edge to create aggregates at the drop edge. An optical microscopic image is given to show the PDI-Hm aggregate coffee ring (boundaries of the PDI-Hm coffee ring are marked with dotted white lines).